

# A new method to calibrate ionospheric pulse dispersion for UHE cosmic ray and neutrino detection using the Lunar Cherenkov technique

R.McFadden<sup>a,\*</sup>, R.Ekers<sup>b</sup>, P.Roberts<sup>b</sup>

<sup>a</sup>ASTRON, 7990 AA Dwingeloo, The Netherlands

<sup>b</sup>CSIRO, Astronomy and Space Science, Epping, NSW 1710, Australia

---

## Abstract

UHE particle detection using the lunar Cherenkov technique aims to detect nanosecond pulses of Cherenkov emission which are produced during UHE cosmic ray and neutrino interactions in the Moon's regolith. These pulses will reach Earth-based telescopes dispersed, and therefore reduced in amplitude, due to their propagation through the Earth's ionosphere. To maximise the received signal to noise ratio and subsequent chances of pulse detection, ionospheric dispersion must therefore be corrected, and since the high time resolution would require excessive data storage this correction must be made in real time. This requires an accurate knowledge of the dispersion characteristic which is parameterised by the instantaneous Total Electron Content (TEC) of the ionosphere. A new method to calibrate the dispersive effect of the ionosphere on lunar Cherenkov pulses has been developed for the LUNASKA lunar Cherenkov experiments. This method exploits radial symmetries in the distribution of the Moon's polarised emission to make Faraday rotation measurements in the visibility domain of synthesis array data (i. e. instantaneously). Faraday rotation measurements are then combined with geomagnetic field models to estimate the ionospheric TEC. This method of ionospheric calibration is particularly attractive for the lunar Cherenkov technique as it may be used in real time to estimate the ionospheric TEC along a line-of-sight to the Moon and using the same radio telescope.

*Keywords:* UHE neutrino detection, Lunar Cherenkov technique, Detectors - telescopes, Ionosphere, Lunar polarisation

---

## 1. Introduction

The lunar Cherenkov technique [1] provides a promising method of UHE neutrino detection since it utilises the lunar regolith as a detector; which has a far greater volume than current ground-based detectors. This technique makes use of Earth-based radio telescopes to detect the coherent Cherenkov radiation emitted when a UHE neutrino interacts in the outer layers of the Moon. It was first applied by Hankins, Ekers and O'Sullivan using the 64-m Parkes radio telescope [2] and significant limits have been already been placed on the UHE neutrino flux by several collaborations [2-6].

Electromagnetic pulses originating in the lunar surface will be dispersed when they arrive at Earth-based receivers due to propagation through the ionosphere which introduces a frequency-dependent time delay. This dispersion reduces the peak amplitude of a pulse, however, dedispersion techniques can be used to recover the full pulse amplitude and consequently increase the chances of detection. Accurate dedispersion requires an understanding of the ionospheric dispersion characteristic and it's effect on radio-wave propagation.

## 2. Effects of Ionospheric Dispersion

The ionosphere is a weakly ionized plasma which is formed by ultraviolet ionizing radiation from the sun. Due to its relationship with the sun, the ionosphere's electron density experiences a strong diurnal cycle and is also dependent on the season of the year, the current phase of the 11-year solar cycle and the geometric latitude of observation. The differential additive delay, caused by pulse dispersion, is parameterised by the ionospheric TEC (see Equation 1)

$$\Delta t = 0.00134 \times STEC \times (\nu_{lo}^{-2} - \nu_{hi}^{-2}), \quad (1)$$

where  $\Delta t$  is the duration of the dispersed pulse in seconds,  $STEC$  is the Slant Total Electron Content in electrons per  $\text{cm}^2$  and  $\nu_{lo}$  and  $\nu_{hi}$  are the receiver bandwidth band edges in Hz.

Cherenkov emission produces a sub-nanosecond pulse and therefore detection requires gigahertz bandwidths to achieve the high time resolution needed to optimise the signal to noise. Due to excessive data storage requirements, the only way to exploit such high data rates is to implement real-time dedispersion and detection algorithms and to store potential events at full bandwidth for later processing. This requires an accurate knowledge of the real-time ionospheric TEC.

---

\*Principal corresponding author

Email address: mcfadden@astron.nl (R.McFadden)

Ionospheric dispersion also offers some potential experimental advantages, particularly for single dish experiments which can not use array timing information to discriminate against RFI. A lunar pulse will travel a one-way path through the ionosphere and be dispersed according to the current ionospheric TEC. Conversely, terrestrial RFI will not be dispersed at all and any Moon-bounce RFI will travel a two-way path through the ionosphere and be dispersed according to twice the current ionospheric TEC. Therefore performing real-time ionospheric dedispersion will optimise detection for lunar pulses and provide discrimination against RFI. Dispersion may also be seen to offer an increase in dynamic range. If triggering is performed on a dedispersed data stream while the raw data is buffered, any pulse clipping that occurs in the triggering hardware can be recovered during offline processing by reconstructing the pulse from the raw, undispersed data.

### 3. Dedispersion Hardware

Pulse dispersion can be corrected using matched filtering techniques implemented in either analog or digital technology. Early LUNASKA experiments made use of the Australia Telescope Compact Array (ATCA) which consists of six 22-m dish antennas. Three antennas were fitted with custom-designed hardware for the neutrino detection experiments and pulse dedispersion was achieved through the use of innovative new analog dedispersion filters that employ a method of planar microwave filter design based on inverse scattering [7].

As the microwave dedispersion filters have a fixed dedispersion characteristic, an estimate had to be obtained for the TEC which would minimise errors introduced by temporal ionospheric fluctuations. The ATCA detection experiments were performed in 2007 and 2008 during solar minimum and therefore relatively stable ionospheric conditions. Initial observations were during the nights of May 5, 6 and 7, 2007 and these dates were chosen to ensure that the Moon was at high elevation (particularly during the night-time hours of ionospheric stability) and positioned such that the ATCA would be sensitive to UHE particles from the galactic center. The filter design was based on predictions made using dual-frequency GPS data and assumed a differential delay of 5 ns across the 1.2–1.8 GHz bandwidth. Data available post experiment revealed that the average differential delay for these nights was actually 4.39 ns, with a standard deviation of 1.52 ns.

The ionosphere experiences both temporal and spatial fluctuations in TEC and therefore some signal loss is expected with a fixed dedispersion filter. A promising digital solution to overcome these losses lies in the use of high speed Field Programmable Gate Arrays (FPGAs). An FPGA implementation allows the dedispersion characteristic to be tuned in real time to reflect temporal changes in the ionospheric TEC. A fully coherent or predetection dedispersion method was pioneered by Hankins and Rickett [8, 9] which completely eliminates the effect of disper-

sive smearing. This is achieved by passing the predetected signal through an inverse ionosphere filter which can be implemented in either the time domain, as an FIR filter, or in the frequency domain.

In 2009, the LUNASKA collaboration started a series of UHE neutrino detection experiments using the 64-m Parkes radio telescope. For these experiments, dedispersion was achieved via a suite of FIR filters implemented on a Vertex 4 FPGA. As GPS TEC estimates are currently not available in real-time, near real-time TEC measurements were derived from foF2 ionosonde measurements. Ionosondes probe the peak transmission frequency (fo) through the F2-layer of the ionosphere which is related to the ionospheric TEC squared. A comparison to GPS data available post-experiment revealed that the foF2-derived TEC data consistently underestimated the GPS TEC measurements. This is attributed to the ground-based ionosondes probing mainly the lower ionospheric layers and not properly measuring TEC contribution from the plasmasphere [10].

### 4. Monitoring the Ionospheric TEC

Coherent pulse dedispersion requires an accurate knowledge of the ionospheric dispersion characteristic which is parameterised by the instantaneous ionospheric TEC.

TEC Measurements can be derived from dual-frequency GPS signals and are available online from NASA’s CDDIS [11], however, these values are not available in real time. The CDDIS TEC data is sampled at two-hour intervals and is currently published after at least a few days delay. Estimates derived from foF2 ionosonde measurements are available hourly from the Australian Ionospheric Prediction Service [12]. However, as discussed, there are known inaccuracies in the derivation of the foF2-based TEC estimates.

Both of these products are published as vertical TEC (VTEC) maps which must be converted to Slant TEC (STEC) estimates to obtain the true total electron content through the slant angle line-of-sight to the Moon. To perform this conversion, the ionosphere can be modeled as a Single Layer Model (SLM) [13] which assumes all free electrons are concentrated in an infinitesimally thin shell and removes the need for integration through the ionosphere. Slant and vertical TEC are related via

$$STEC = F(z)VTEC. \quad (2)$$

where  $F(z)$  is a slant angle factor defined as

$$F(z) = \frac{1}{\cos(z')} \quad (3)$$

$$= \frac{1}{\sqrt{1 - \left(\frac{R_e}{R_e + H} \sin(z)\right)^2}}, \quad (4)$$

$R_e$  is the radius of the Earth,  $z$  is the zenith angle to the source and  $H$  is the height of the idealised layer above the Earth's surface (see Figure 1). The CDDIS also use an SLM ionosphere for GPS interpolation algorithms and assume a mean ionospheric height of 450 km.

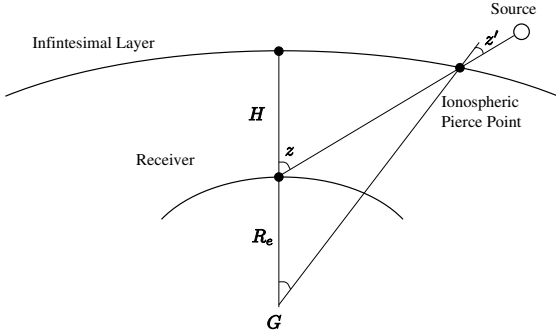


Figure 1: Parameters of the Ionospheric Single Layer Model.

## 5. A New Method of Ionospheric Calibration

As the solar cycle enters a more active phase accurate pulse dedispersion is becoming a more important experimental concern for the lunar Cherenkov technique. This requires methods of obtaining more accurate measurements of the ionospheric TEC.

A new technique has been formulated to obtain TEC measurements that are both instantaneous and line-of-sight to the Moon. The ionospheric TEC can be deduced from Faraday rotation measurements of a polarised source combined with geomagnetic field models, which are more stable than ionospheric models (the CDDIS [11] states that ionospheric TEC values are accurate to  $\sim 20\%$  while the IGRF [14] magnetic field values are accurate to better than 0.01%). Lunar thermal emission can be used as the polarised source since Brewster angle effects produce a nett polarisation excess in the emission from the lunar limb [15]. This provides a method for calibrating the ionosphere directly line-of-sight to the Moon and makes the lunar Cherenkov technique extremely attractive for UHE cosmic ray and neutrino astronomy as it allows the characteristic dispersion to be used as a powerful discriminant against terrestrial RFI whilst removing the need to search in dispersion-space.

The unique constraints of an UHE neutrino detection experiment using the lunar Cherenkov technique conflict with traditional methods of planetary synthesis imaging and polarimetry which requires a complete set of spacings and enough observing time for earth rotation. Therefore to apply this method of ionospheric calibration to the ATCA detection experiments, innovations in the analysis of lunar polarisation observations were required. In particular, a method of obtaining lunar Faraday rotation estimates in the visibility domain (i. e. without Fourier inversion to the image plane) had to be developed.

Working in the visibility domain removes both the imaging requirement of a compact array configuration, which would increase the amount of correlated lunar noise between receivers, and also removes the need for earth rotation allowing measurements to be obtained in real time. This technique makes use of the angular symmetry in planetary polarisation distribution. The intrinsic thermal radiation of a planetary object appears increasingly polarised toward the limb, when viewed from a distant point such as Earth [15, 16]. The polarised emission is radially aligned and is due to the changing angle of the planetary surface toward the limb combined with Brewster angle effects. The angular symmetry of this distribution can be exploited by an interferometer so that an angular spatial filtering technique may be used to obtain real-time position angle measurements directly in the visibility domain. The measured position angles are uniquely related to the corresponding  $uv$  angle at the time of the observation. Comparison with the expected radial position angles, given the current  $uv$  angle of the observation, gives an estimate of the Faraday rotation induced on the Moon's polarised emission. Faraday rotation estimates can be combined with geomagnetic field models to determine the associated ionospheric TEC and subsequently provide a method of calibrating the current atmospheric effects on potential Cherenkov pulses.

Observations of the Moon were taken using the 22-m telescopes of the Australia Telescope Compact Array with a center frequency of 1384 MHz. At this frequency the Moon is in the near field of the array, however, investigation of the Fresnel factor in polar coordinates showed that it has no dependence on the spatial parameter, which determines the polarisation distribution of a planetary body.

Using the angular spatial filtering technique, position angle estimates were calculated directly in the visibility domain of the lunar observational data. The Faraday rotation estimates were obtained by comparing these angles to the instantaneous  $uv$  angle and the resultant Faraday rotation estimates were averaged over small time increments to smooth out noise-like fluctuations. Since the polarised lunar emission received on each baseline varied in intensity over time, there were nulls during which the obtained position angle information was not meaningful. A threshold was applied to remove position angle measurements taken during these periods of low polarised intensity and baseline averaging was considered necessary as the results on each baseline were slightly different and each affected differently by intensity nulls. The Faraday rotation estimates were converted to estimates of ionospheric TEC via

$$\Omega = 2.36 \times 10^4 \nu^{-2} \int_{\text{path}} N(s) B(s) \cos(\theta) ds, \quad (5)$$

where  $\Omega$  is the rotation angle in radians,  $f$  is the signal frequency in Hz,  $N$  is the electron density in  $\text{m}^3$ ,  $B$  is the geomagnetic field strength in T,  $\theta$  is the angle between the direction of propagation and the magnetic field vector and  $ds$  is a path element in m.

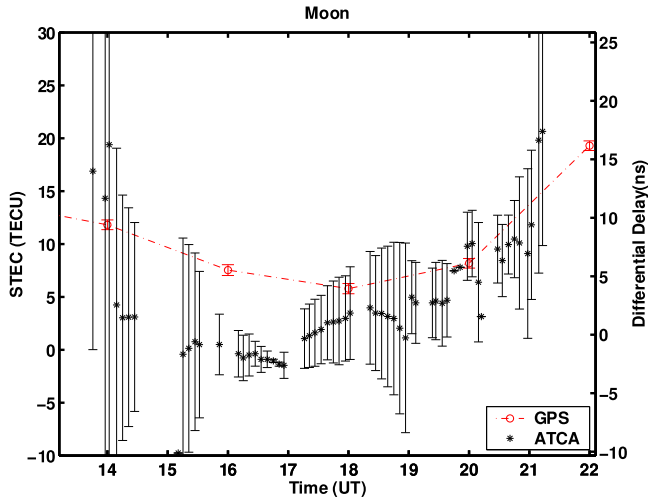


Figure 2: Lunar Faraday rotation estimates converted to (left) ionospheric TEC values and (right) the differential delay across 1.2–1.8 GHz.

To evaluate the effectiveness of this new ionospheric calibration technique, the TEC results were compared against ionospheric TEC estimates derived from dual-frequency GPS data (Figure 2). Slant angle factors were used to convert the GPS VTEC estimates to STEC toward the Moon for comparison with the ATCA data. Both data sets exhibited a similar general trend of symmetry around the Moon’s transit. However, the ATCA data often underestimated the GPS data, particularly around 14:30–17:00 UT where the STEC estimates may have been influenced by bad data from the shorter baselines or due to TEC contribution from the plasmasphere which is not in the presence of a magnetic field [10]. These observations were taken when the TEC was very low and therefore the relative error in the TEC estimates is large.

## 6. Conclusions

As the sun enters a more active phase, accurate ionospheric pulse dispersion is becoming a more important experimental concern for UHE neutrino detection using the lunar Cherenkov technique. Hardware dedispersion options rely on the accuracy of real-time ionospheric TEC measurements and, while there are a few options available for obtaining these measurements, they are not currently available in real time nor directly line-of-sight to the Moon. A new ionospheric calibration technique has been developed. This technique uses Faraday rotation measurements of the polarised thermal radio emission from the lunar limb combined with geomagnetic field models to obtain estimates of the ionospheric TEC which are both instantaneous and line-of-sight to the Moon. STEC estimates obtained using this technique have been compared to dual-frequency GPS data. Both data sets exhibited similar features which can be attributed to ionospheric events,

however, more observations are required to investigate this technique further.

## 7. Acknowledgements

This research was supported as a Discovery Project by the Australian Research Council. The Compact Array and Parkes Observatory are part of the Australia Telescope which is funded by the Commonwealth of Australia for operation as a National Facility managed by CSIRO.

## References

- [1] R. D. Dagkesamanskii, I. M. Zheleznykh, A radio astronomy method of detecting neutrinos and other superhigh-energy elementary particles, *PAZh* 50 (1989) 233.
- [2] T. H. Hankins, R. D. Ekers, J. D. O’Sullivan, A search for lunar radio Cherenkov emission from high-energy neutrinos, *MNRAS* 283 (1996) 1027.
- [3] P. W. Gorham, C. L. Hebert, K. M. Liewer, C. J. Naudet, D. Saltzberg, D. Williams, Experimental Limit on the Cosmic Diffuse Ultrahigh Energy Neutrino Flux, *Phys. Rev. Lett.* 93 (4) (2004) 041101. [arXiv:astro-ph/0310232](https://arxiv.org/abs/astro-ph/0310232), [doi:10.1103/PhysRevLett.93.041101](https://doi.org/10.1103/PhysRevLett.93.041101).
- [4] A. R. Beresnyak, R. D. Dagkesamanskii, I. M. Zheleznykh, A. V. Kovalenko, V. V. Oreshko, Limits on the Flux of Ultrahigh-Energy Neutrinos from Radio Astronomical Observations, *Astronomy Reports* 49 (2005) 127. [doi:10.1134/1.1862359](https://doi.org/10.1134/1.1862359).
- [5] C. W. James, R. J. Protheroe, R. D. Ekers, J. Alvarez-Muñiz, R. A. McFadden, C. J. Phillips, P. Roberts, J. D. Bray, LUNASKA experiment observational limits on UHE neutrinos from Centaurus A and the Galactic Centre, *MNRAS* (2010) 1425 [arXiv:0906.3766](https://arxiv.org/abs/0906.3766), [doi:10.1111/j.1365-2966.2010.17486.x](https://doi.org/10.1111/j.1365-2966.2010.17486.x).
- [6] S. Buitink, O. Scholten, J. Bacelar, R. Braun, A. G. de Bruyn, H. Falcke, K. Singh, B. Stappers, R. G. Strom, R. a. Yahyaoui, Constraints on the flux of Ultra-High Energy neutrinos from WSRT observations, *ArXiv e-prints* [arXiv:1004.0274](https://arxiv.org/abs/1004.0274).
- [7] P. Roberts, G. Town, Design of microwave filters by inverse scattering, *IEEE Transactions on Microwave Theory and Techniques* 43 (4 Part 1) (1995) 739.
- [8] T. H. Hankins, Microsecond Intensity Variations in the Radio Emissions from CP 0950, *ApJ* 169 (1971) 487. [doi:10.1086/151164](https://doi.org/10.1086/151164).
- [9] T. H. Hankins, B. J. Rickett, Pulsar signal processing, in: *Methods in Computational Physics. Volume 14 - Radio astronomy*, Vol. 14, 1975, p. 55.
- [10] J. E. Titheridge, Determination of ionospheric electron content from the Faraday rotation of geostationary satellite signals, *Planet. Space Sci.* 20 (3) (1972) 353.
- [11] NASA, Crustal Dynamics Data Information System., [http://cddisa.gsfc.nasa.gov/gnss\\_datasum.html](http://cddisa.gsfc.nasa.gov/gnss_datasum.html).
- [12] Ionospheric Prediction Service, Australasia Total Electron Content., <http://www.ips.gov.au/Satellite/2/1/11>.
- [13] S. Todorova, T. Hobiger, H. Schuh, Using the Global Navigation Satellite System and satellite altimetry for combined Global Ionosphere Maps, *Advances in Space Research* 42 (2008) 727–736. [doi:10.1016/j.asr.2007.08.024](https://doi.org/10.1016/j.asr.2007.08.024).
- [14] British Geological Survey, The International Geomagnetic Reference Field Model., <http://www.geomag.bgs.ac.uk/gifs/igrf.html>.
- [15] C. E. Heiles, F. D. Drake, On the polarization and intensity of thermal radiation from a planetary surface, *Icarus* 2 (1963) 281.
- [16] S. Poppi, E. Carretti, S. Cortiglioni, V. D. Krotikov, E. N. Vinyajkin, The Moon as a calibrator of linearly polarized radio emission for the SPORt project, in: S. Cecchini, S. Cortiglioni, R. Sault, C. Sbarra (Eds.), *Astrophysical Polarized Backgrounds*, Vol. 609 of American Institute of Physics Conference Series, 2002, p. 187.